RSC Advances

PAPER

View Article Online
View Journal | View Issue

Cite this: *RSC Adv.*, 2017, **7**, 37261

Cobalt(II)-8-hydroxyquinoline-5-sulfonic acid complex/*N*-(4-aminobutyl)-*N*-ethylisoluminol/reduced graphene hybrids as nanocatalytic reaction platforms for chemiluminescence†

Qi Li, ‡ Xiangyang Liu,‡ Meng Zhuang, Xu Wang and Hua Cui *

In this work, we report a novel GO-based hybrid consisting of *N*-(4-aminobutyl)-*N*-ethylisoluminol (ABEI), a cobalt(II)-8-hydroxyquinoline-5-sulfonic acid complex ($Co^{II}(HQS)_2$) and reduced GO hybrids ($Co^{II}(HQS)_2$/ABEI/rGO) with good stability and easy purification *via* a facile strategy by virtue of π–π stacking and coordination, which could be used as an excellent nanocatalytic reaction platform for chemiluminescence (CL) when reacted with hydrogen peroxide, dissolved oxygen and periodate in alkaline solution. This was attributed to the fact that $Co^{II}(HQS)_2$ catalyzed the generation of reactive radicals such as $HO^{\bullet}$, $O_2^{\bullet-}$, and periodate anion radicals (I^{VI}) and π-conjugated carbon radicals (π–C=C$^{\bullet}$) as well as $ABEI^{\bullet-}$ on the GO surface. GO as a reaction platform facilitated the reaction of $ABEI^{\bullet-}$ with $O_2^{\bullet-}$ to produce intensive CL. It was also found that there was a dilution-initiated CL enhancement in $Co^{II}(HQS)_2$/ABEI/rGO–H_2O_2 system but not in the $Co^{II}(HQS)_2$/ABEI/rGO–O_2 and $Co^{II}(HQS)_2$/ABEI/rGO–KIO_4 systems. This was due to the competition of the dilution-decreased reduced GO quenching effect and dilution-decreased $Co^{II}(HQS)_2$ concentration. This work provides new insight into the physicochemical properties of functionalized GO hybrids and excellent nanocatalytic platforms for CL reactions, which may find future applications in bioassays, biosensors, bioimaging and microchips.

Received 6th June 2017
Accepted 23rd July 2017

DOI: 10.1039/c7ra06327j

rsc.li/rsc-advances

Introduction

Nanomaterials as catalysts in chemiluminescence (CL) reactions have enjoyed great attention owing to their important potential applications in sensors, catalysts, bioassays and biological imaging.[1–4] Since Zhang and coworkers first reported the catalysis of gold nanoparticles (AuNPs) in luminol CL reactions,[5] studies on nanomaterial-catalyzed CL reactions have been extended to various nanomaterials, such as AgNPs,[6] PtNPs,[7] ZnO NPs,[8] *etc.* Such nanomaterials as nanosized platforms could effectively facilitate the formation of reactive radicals and electron transfer, leading to strong light emission.[5] In the above work, CL reagents existed in liquid-phase in the CL reactions. Subsequently, it was found that CL efficiency could be improved when CL reagents were directly immobilized on the surface of nanomaterials due to the enhanced electron transfer ability on the surface of the nanointerface.[9] These CL functionalized nanomaterials have been successfully used as nanoprobes and nanointerfaces for label-based and label-free bioassays.[10–12] Furthermore, in order to further improve CL efficiency, both of CL reagent and catalyst (include metal ions, metal complexes and molecules) were immobilized on the surface of nanomaterials. Unique CL emission was observed on nanocatalytic reaction platform due to synergistic effect of nanomaterials, catalysts and CL reagents occurred on such heterogeneous nanointerface. For examples, CL reagent *N*-(4-aminobutyl)-*N*-ethylisoluminol (ABEI) and catalyst cobalt complexes were successfully grafted on the surface of gold nanoparticles, which exhibited excellent CL and electrochemiluminescence (ECL) activity and was used for the determination of specific DNA sequence related to diseases.[13,14] Graphene and graphene oxide (GO) with a single atomic layer of sp^2 carbon atoms and high surface-to-volume ratio could be also used as nanocatalytic reaction platforms for CL reactions.[15,16] Later on, ABEI and catalyst bifunctionalized GO or graphene hybrids with higher CL efficiency, including ABEI/hemin bifunctionalized GO and ABEI/horseradish peroxidase bifunctionalized GO, have been developed.[17,18] However, nanocatalytic reaction platforms were restricted to the reactions of luminol-type CL reagents with H_2O_2 and nanocatalytic reaction platforms for various CL reactions are far from fully developed.

In this work, we report a novel GO-based hybrid with good stability and easy purification consisting of ABEI, $Co^{II}(HQS)_2$

CAS Key Laboratory of Soft Matter Chemistry, Collaborative Innovation Center of Chemistry for Energy Materials, Department of Chemistry, University of Science and Technology of China, Hefei, Anhui 230026, P. R. China. E-mail: hcui@ustc.edu.cn; Fax: +86 551 63600730; Tel: +86 551 63600730

† Electronic supplementary information (ESI) available. See DOI: 10.1039/c7ra06327j

‡ The authors are co-first authors and contributed equally to this work.

and reduced GO hybrids ($Co^{II}(HQS)_2$/ABEI/rGO) *via* a facile strategy. The as-prepared $Co^{II}(HQS)_2$/ABEI/rGO hybrids were characterized by atomic force microscopy (AFM), UV-vis absorption spectra, fluorescence spectra (FL), Raman spectra, X-ray photoelectron spectroscopy (XPS) and atomic emission spectrophotometry (ICP-AES). And the assembly mechanism was discussed. It was found that the as-prepared $Co^{II}(HQS)_2$/ABEI/rGO could be used as excellent nanocatalytic reaction platforms for CL when reacted with hydrogen peroxide, the dissolved oxygen and periodate in alkaline solution. The mechanism of various CL reactions was explored. Moreover, the effect of dilution on CL behavior of various CL reactions was studied and related mechanism was discussed.

Experimental section

Chemicals and materials

Graphite oxide was purchased from XFNANO Materials Tech Co., Ltd. (Nanjing, China). *N*-(4-Aminobutyl)-*N*-ethylisoluminol (ABEI) (TCI, Japan) without further purification was dissolved in 0.1 M NaOH solution to prepare a 10 mM stock solution of ABEI. 8-Hydroxyquinoline-5-sulphonic (HQS) was purchased from J&K Scientific Ltd. (Shanghai, China). Cobalt(II) chloride hexahydrate, ammonia, hydrazine, and potassium periodate (KIO_4) were purchased form Sinopharm Chemical Reagent Co. Ltd (Shanghai, China). Working solutions of H_2O_2 were prepared fresh daily from 30% (v/v) H_2O_2 (Xinke Electrochemical Reagent Factory, Bengbu, China). All other reagents were of analytical grade. Ultrapure water was prepared by a Milli-Q system (Millipore, France) and was used throughout.

Preparation of $Co^{II}(HQS)_2$/ABEI/rGO

Firstly, 0.1 mg mL^{-1} GO aqueous dispersion was obtained from graphite oxide by ultrasonic for 2 hours. Then 1 mL of 10 mM ABEI in NaOH solution was added to 100 mL of 0.1 mg mL^{-1} GO aqueous dispersion. After sonication for 10 min, the mixture was vigorously stirred at 80 °C for 24 h to obtain the ABEI/GO. For the preparation of $Co^{II}(HQS)_2$ complex, 23.8 mg $CoCl_2 \cdot 6H_2O$ was added into 100 mL of 2 mM HQS alkaline solution containing 0.005 M NaOH. The above solutions were mixed, stirred and heated for about an hour at 60 °C to form a yellow and transparent solution. Next, 1 mL of $Co^{II}(HQS)_2$ complex solution and 200 μL of ammonia solution were added into 100 mL of the as-prepared ABEI/GO solution, followed by the addition of 30 μL of hydrazine solution. Then the mixture was vigorously stirred at 60 °C for 4 h. After twice centrifugation and redispersion, $Co^{II}(HQS)_2$/ABEI/rGO hybrids were obtained.

Characterization of $Co^{II}(HQS)_2$/ABEI/rGO hybrids

The morphology and surface composition of as-prepared $Co^{II}(HQS)_2$/ABEI/rGO hybrids were characterized by UV-visible spectra (Agilent 8453 UV-visible spectrophotometer, USA), Raman spectra (LabRamHR, JobinYvon, France), AFM (Multimode V, Veeco), XPS (VG Scientific, UK) with Al Kα radiation as the X-ray source and ICP-AES (Optima 7300 DV, PerkinElmer, US).

CL measurements

The CL property of $Co^{II}(HQS)_2$/ABEI/rGO hybrids was studied by static injection CL system with a centro LB 960 microplate luminometer (Berthold, Germany). For the CL reactions of $Co^{II}(HQS)_2$/ABEI/rGO hybrids with oxidant H_2O_2, O_2 and KIO_4, 50 μL of purified $Co^{II}(HQS)_2$/ABEI/rGO was first added into the wells of 96-well plates and then 50 μL of oxidant was injected into the wells, CL signals were produced and recorded. CL spectra were measured on a FL spectrometer (HITACHI F-7000, Hitachi, Japan) operated with the lamp off.

Results and discussion

Preparation and characterization of $Co^{II}(HQS)_2$/ABEI/rGO

The preparation of $Co^{II}(HQS)_2$/ABEI/rGO hybrids is depicted in Scheme 1. First, ABEI molecules were mixed with GO at 80 °C for 24 hours to produce ABEI/GO hybrids. Second, $Co^{II}(HQS)_2$ complex reacted with ABEI/GO hybrids in the presence of ammonia and hydrazine to obtain $Co^{II}(HQS)_2$/ABEI/rGO hybrids. The as-prepared $Co^{II}(HQS)_2$/ABEI/rGO hybrids easy separated from precursor exhibited good stability and water-solubility.

The morphology of the as-prepared $Co^{II}(HQS)_2$/ABEI/rGO hybrids was investigated by AFM. The AFM images with a height profile are shown in Fig. 1. The morphology of $Co^{II}(HQS)_2$/ABEI/rGO is the same with that of GO and ABEI/GO, which is cast on a mica wafer with essentially single-layered carbon structure. These results indicate that the as-prepared $Co^{II}(HQS)_2$/ABEI/rGO hybrids remain dispersive. The thickness of GO measured from the height profile of the AFM image is about 0.76 nm, which is consistent with the data reported in the literature.[19] After functionalized with ABEI, the height of ABEI/GO sheet shows a 0.14 nm increment. The thickness of $Co^{II}(HQS)_2$/ABEI/rGO is about 1.15 nm, indicating that ABEI molecule and $Co^{II}(HQS)_2$ complex are assembled on the surface of graphene sheet.

The composition of the as-prepared $Co^{II}(HQS)_2$/ABEI/rGO was studied by XPS, ICP-AES, UV-vis and Raman spectra. XPS

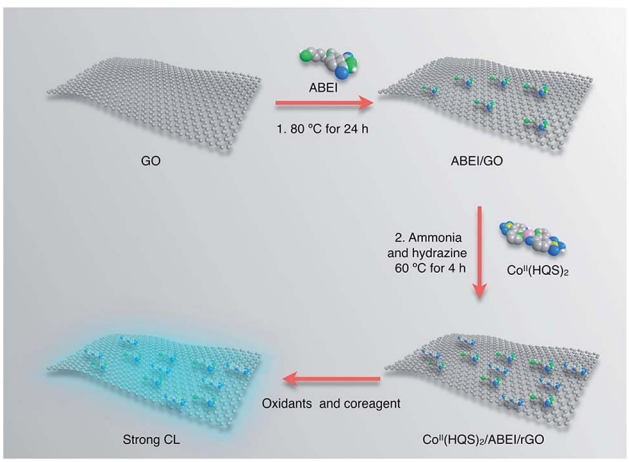

Scheme 1 Illustration of preparation of $Co^{II}(HQS)_2$/ABEI/rGO hybrids.

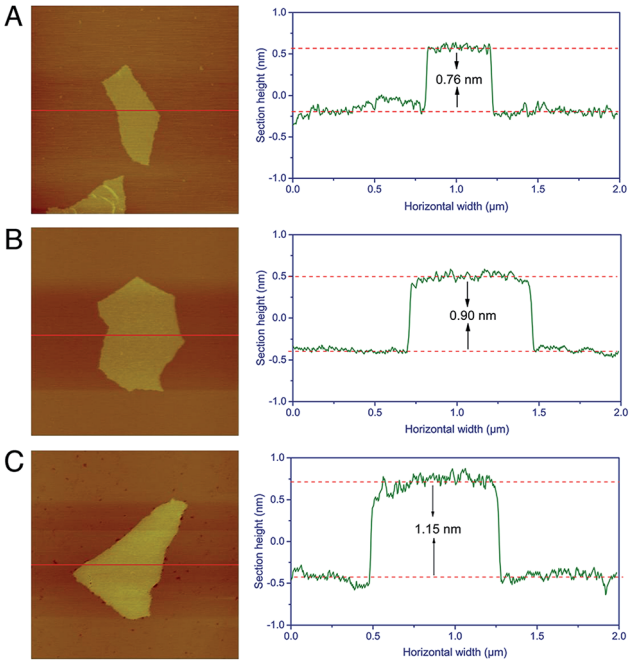

Fig. 1 Tapping mode AFM images with height profile (green curves) taken along the red line of (A) exfoliated GO, (B) ABEI/GO and (C) $Co^{II}(HQS)_2$/ABEI/rGO.

of $Co^{II}(HQS)_2$/ABEI/rGO is shown in Fig. 2, C 1s/O 1s ratio obtained from the XPS survey spectrum increased after ABEI and $Co^{II}(HQS)_2$ were connected to the surface of GO successively. Compared with GO, the C 1s spectrum of $Co^{II}(HQS)_2$/ABEI/rGO showed a great decrease at 286.4 eV and 287.2 eV. The results strongly supported that the GO in $Co^{II}(HQS)_2$/ABEI/rGO was partially reduced. The N 1s spectrum of $Co^{II}(HQS)_2$/ABEI/rGO was curved-fitted into three components at 399.5, 400.7 and 401.8 eV, which were contributed to the –N–sp^3C, –N–sp^2C and quaternary N, respectively.[20] Compared with the N 1s spectrum of GO, the survey of $Co^{II}(HQS)_2$/ABEI/rGO and ABEI/GO showed a new peak at 400.7 eV originating from the –N–CO– group in ABEI. And the N 1s peak at 399.5 eV increased due to the –N–sp^3C from ABEI. Hence, the results indicated that the ABEI existed on the surface of ABEI/GO and $Co^{II}(HQS)_2$/ABEI/rGO. The XPS spectra of $Co^{II}(HQS)_2$/ABEI/rGO demonstrated the existence of S 2p and Co 2p binding energy, which were absent in the survey spectrum of ABEI/GO (Fig. S1†). The Co 2p spectrum was curved-fitted into four components at 796.7, 781.0, 801.2 and 785.8 eV, which was attributed to the $2p_{1/2}$, $2p_{3/2}$ spin–orbit and the satellite lines for the high spin Co(II), respectively.[21] The results indicated that $Co^{II}(HQS)_2$ complex existed on the surface of GO sheets and cobalt was mainly Co(II). Furthermore, the amount of Co(II) was calculated as 0.33 μg mL^{-1} by ICP-AES. As shown in Fig. S2,† UV-vis spectra also supported the presence of ABEI molecules and $Co^{II}(HQS)_2$ complex and on the surface of $Co^{II}(HQS)_2$/ABEI/rGO. Raman spectra were also used to monitor the structural changes during the synthesis of $Co^{II}(HQS)_2$/ABEI/rGO from GO. It was reported that the intensity of the D Raman band was a marker of the defect density and the I(D)/I(G) ratio was an important parameter to characterize graphene defect density.[22] As shown in Fig. S3,† the I(D)/I(G) ratio was in the order: $Co^{II}(HQS)_2$/ABEI/rGO > ABEI/GO > GO. The results also indicated that GO were deoxygenated in $Co^{II}(HQS)_2$/ABEI/rGO, which was in good agreement with the XPS results.

The assembly mechanism of $Co^{II}(HQS)_2$/ABEI/rGO was investigated. Our previous work suggested that ABEI was attached to graphene *via* π–π interaction.[23] HQS was used as a ligand with great complexation constants and water solubility, which could complex with metal ion through N atoms and deprotonated quinolinol-O atoms.[24,25] In this case, cobalt(II) ion could also complex with HQS to form a 1 : 2 complex with an octahedral coordination structure. In the equatorial positions, Co^{2+} are coordinated by the N and O atoms of the quinolinol moiety to form a planar structure. Due to the π-conjugated quinolinol group, $Co^{II}(HQS)_2$ might be assembled to the surface of GO *via* π–π stacking. On the other hand, O atom from GO

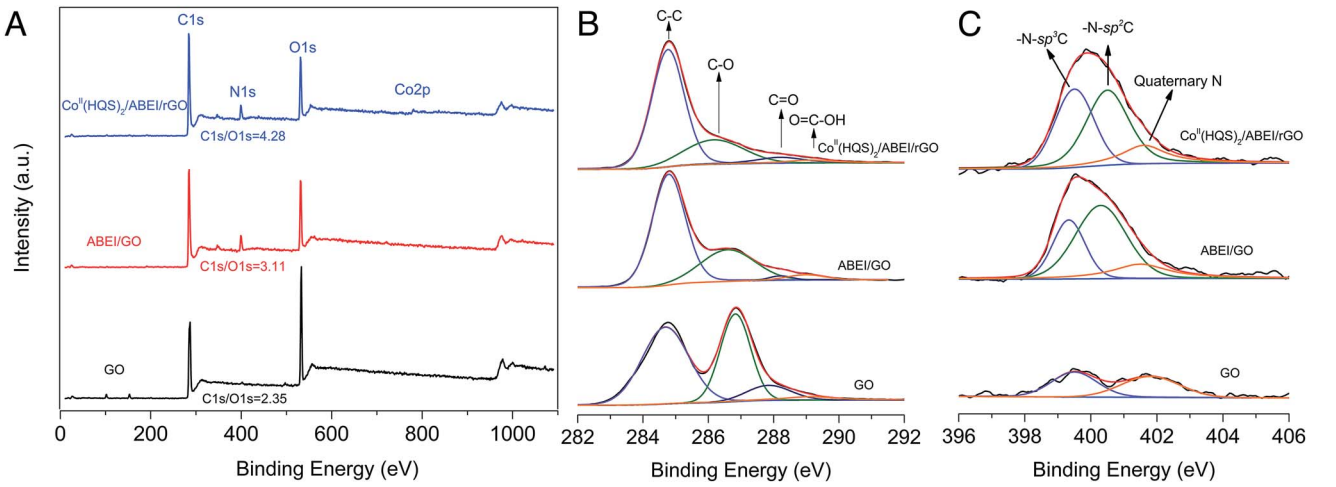

Fig. 2 Survey XPS data of (A) GO, ABEI/GO and $Co^{II}(HQS)_2$/ABEI/rGO. XPS survey of (B) C 1s and (C) N 1s from GO, ABEI/GO and $Co^{II}(HQS)_2$/ABEI/rGO, respectively.

might coordinate with Co^{2+} *via* the axial position.[26] Accordingly, $Co^{II}(HQS)_2$ complex might be absorbed on the surface of GO sheets *via* π–π stacking and coordination between $Co^{II}(HQS)_2$ and GO as shown in Fig. S4.†

CL behavior in hydrogen peroxide system

The CL behavior of $Co^{II}(HQS)_2$/ABEI/rGO hybrids with H_2O_2 in alkaline solution was investigated. As shown in Fig. 3, it can be seen that $Co^{II}(HQS)_2$/ABEI/rGO (black line) exhibited excellent CL activity, which was ~70 times higher than that of ABEI/GO (green line) and the CL kinetic curve showed a typical flash light emission. In addition, the synthesis dosage of ABEI in the hybrids is about 1/18 of that used in previously reported ABEI functionalized rGO hybrids.[17,23] The results revealed that the incorporation of $Co^{II}(HQS)_2$ into ABEI/GO to form a novel bifunctionalized GO hybrids could highly improve the CL activity. As shown in Fig. S5,† the maximum CL emission wavelength of $Co^{II}(HQS)_2$/ABEI/rGO–H_2O_2 was centered at ~440 nm, which was consistent with that of ABEI with H_2O_2. Thus, the CL emission was from the reaction of ABEI on the surface of $Co^{II}(HQS)_2$/ABEI/rGO with H_2O_2. As shown in Fig. S6,† the effects of pH and concentration of H_2O_2 on the CL reaction between $Co^{II}(HQS)_2$/ABEI/rGO and H_2O_2 were investigated. The CL intensity increased with the increase of pH. And the logarithm of integrated of CL intensity increased linearly with the logarithm of the concentration of H_2O_2 in the range of 0.1 μM to 0.5 mM. The results indicated that higher alkaline condition and H_2O_2 concentration are advantageous to the CL reaction in $Co^{II}(HQS)_2$/ABEI/rGO–H_2O_2 system, which was consistent with the CL mechanism of cyclic hydrazides.[27,28] The decomposition of H_2O_2 would generate hydroxyl radicals ($HO^{\bullet}$) and superoxide radicals ($O_2^{\bullet-}$), which could react with ABEI to produce CL. The higher pH could accelerate the decomposition of H_2O_2 and the deprotonation of the excited state oxidation product of ABEI (ABEI-OX*) and generate higher CL emission. Finally, 0.1 mM H_2O_2 (pH 12) was recommended as optimized conditions for the CL because higher solution pH would corrode the injector of luminometer and higher concentration of H_2O_2 would cause poor stability.

Furthermore, the CL enhancement of $Co^{II}(HQS)_2$ and GO in ABEI–H_2O_2 system was investigated. The addition of HQS only affect slightly the CL kinetic curve. When $Co^{II}(HQS)_2$ aqueous solution was added into ABEI/GO dispersion, strong CL emission was observed as shown in Fig. 3 (red line). The result indicated that $Co^{II}(HQS)_2$ as an efficient catalyst could increase the rate of CL reaction and thereby greatly increased the CL intensity. Earlier studies showed that Co^{2+} could interact with H_2O_2 to rapidly generate $HO^{\bullet}$ and $O_2^{\bullet-}$.[29,30] N. V. Thakkar and coworkers reported that the complexation of Co^{2+} have enhanced effect on the catalytic of decomposition of H_2O_2.[31,32] $Co^{II}(HQS)_2$ complex might have similar enhanced catalytic effect on the decomposition of H_2O_2 to facilitate the formation of $HO^{\bullet}$ and $O_2^{\bullet-}$. Moreover, the CL intensity obviously increased in an oxygen-saturated solution and decreased in a nitrogen-saturated solution, indicating that the dissolved oxygen (O_2) took part in the CL reaction (Fig. S7A†).

In view of the above discussion, the CL mechanism of $Co^{II}(HQS)_2$/ABEI/rGO with H_2O_2 is summarized in Scheme 2. The immobilized $Co^{II}(HQS)_2$ complex could catalyze the decomposition of H_2O_2 to yield highly reactive $HO^{\bullet}$ and $O_2^{\bullet-}$ radicals on the surface of GO, which reacted with GO to produce π–C=C$^{\bullet}$. Such radicals reacted with ABEI to form ABEI radicals ($ABEI^{\bullet-}$), which further interacted with $O_2^{\bullet-}$ to generate intensive CL emission. The result demonstrated that the $Co^{II}(HQS)_2$ complex and the GO platform exhibited superior catalysis effect in $Co^{II}(HQS)_2$/ABEI/rGO–H_2O_2 system. The as-prepared $Co^{II}(HQS)_2$/ABEI/rGO could act as an effective nanocatalytic reaction platform for the heterogenous CL reaction of ABEI with H_2O_2.

CL behavior in the dissolved oxygen system

It was found that as-prepared $Co^{II}(HQS)_2$/ABEI/rGO could directly react with 0.1 M NaOH solution to produce strong CL emission as shown in Fig. 4 (black line). Controlling experiments were also carried out when 0.1 M NaOH was added to control solutions (Fig. 4). Very weak light emission was observed when ABEI/GO (green line) or the mixture of ABEI/GO with HQS (blue line) was added to 0.1 M NaOH solution. The CL intensity

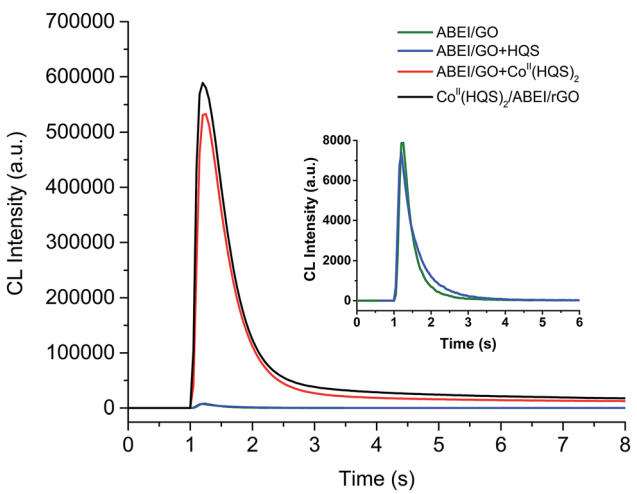

Fig. 3 CL kinetic curves for reaction of ABEI/GO, ABEI/GO mixed with HQS, ABEI/GO mixed with $Co^{II}(HQS)_2$ and $Co^{II}(HQS)_2$/ABEI/rGO with H_2O_2. Reaction conditions: 0.1 mM H_2O_2 in 0.01 M NaOH.

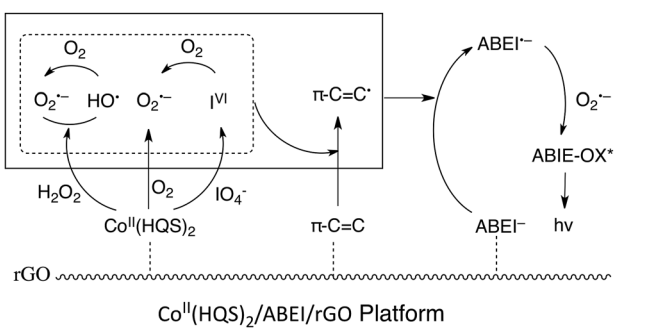

Scheme 2 The CL mechanism of $Co^{II}(HQS)_2$/ABEI/rGO with H_2O_2, dissolved O_2 and IO_4^-.

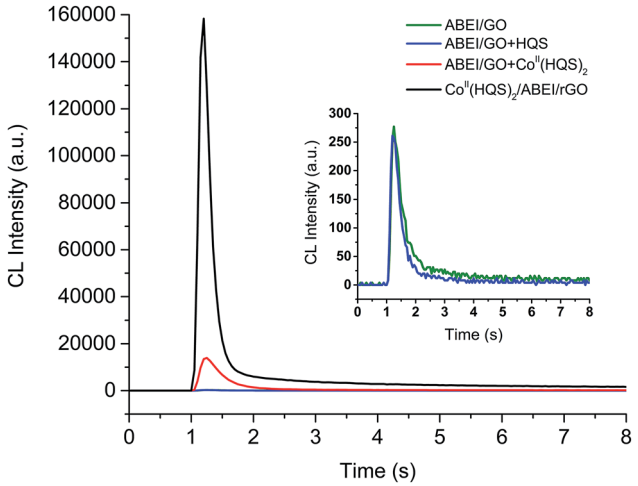

Fig. 4 CL kinetic curves for reaction of ABEI/GO, ABEI/GO mixed with HQS, ABEI/GO mixed with $Co^{II}(HQS)_2$ and $Co^{II}(HQS)_2$/ABEI/rGO with the dissolved oxygen. Reaction conditions: 0.1 M NaOH.

from the mixture of $Co^{II}(HQS)_2$ with ABEI/GO enhanced by 50 times comparing with that of ABEI/GO. The CL intensity of $Co^{II}(HQS)_2$/ABEI/rGO was about 500 times higher than that of ABEI/GO. The immobilization of $Co^{II}(HQS)_2$ complexes on the surface of ABEI/GO resulted in further increase of the CL intensity. Moreover, the maximum emission wavelength of $Co^{II}(HQS)_2$/ABEI/rGO initiated CL was at ~440 nm, indicating that the emitter was the excited state oxidation product of ABEI (Fig. S5C†). It was deduced that the light emission may be due to the reaction of $Co^{II}(HQS)_2$/ABEI/rGO with the dissolved oxygen in alkaline solution. To prove the assumption, the effects of O_2 and N_2 on the $Co^{II}(HQS)_2$/ABEI/rGO CL reaction were investigated. As shown in Fig. S7B,† the CL intensity decreased in a nitrogen-saturated solution and increased in an oxygen-saturated solution, indicating that the dissolved O_2 was involved the CL reaction. $Co^{II}(HQS)_2$/ABEI/rGO reacted with the dissolved O_2 in alkaline solution, leading to CL emission.

The mechanism of $Co^{II}(HQS)_2$/ABEI/rGO–O_2 system was investigated. It was reported that Co^{II} complex could converse the dissolved oxygen to $O_2^{\bullet-}$ in O_2-containing and high alkaline solution.[33] In this case, $Co^{II}(HQS)_2$ may react with the dissolved O_2 in alkaline solution to form $O_2^{\bullet-}$. When the $Co^{II}(HQS)_2$ complexes were immobilized on the surface of ABEI/GO, the CL intensity increased significantly. This was attributed to that $O_2^{\bullet-}$ could react with GO and ABEI to produce π–C=C$^{\bullet}$ and ABEI$^{\bullet-}$ radicals. Finally, $O_2^{\bullet-}$ radicals reacted with ABEI$^{\bullet-}$ to yield CL emission. Thus, the as-prepared $Co^{II}(HQS)_2$/ABEI/rGO could also act as an effective nanocatalytic reaction platform for the heterogenous CL reaction of ABEI with the dissolved oxygen. The possible reaction pathways are also shown in Scheme 2.

CL behavior in periodate system

Unlike H_2O_2, periodate is rather stable oxidant and can oxidize luminol to produce strong CL emission. It was reported that Co^{2+} and Mn^{2+} could catalyze the CL reaction between luminol and KIO_4.[34] Hence, the CL behavior of $Co^{II}(HQS)_2$/ABEI/rGO with KIO_4 was investigated as shown in Fig. 5. The $Co^{II}(HQS)_2$/ABEI/rGO exhibited good CL emission in KIO_4–NaOH system. ABEI/GO and the mixture of ABEI/GO with HQS only demonstrated weak CL emission. The mixture of ABEI/GO with $Co^{II}(HQS)_2$ showed significant CL emission. However, the CL intensity of $Co^{II}(HQS)_2$/ABEI/rGO–KIO_4 was about 150 and 3 times higher than that of ABEI/GO and ABEI/GO + $Co^{II}(HQS)_2$, respectively. As shown in Fig. S5D,† the CL emission peak of $Co^{II}(HQS)_2$/ABEI/rGO–KIO_4 was at ~440 nm, indicating that the emitter was the excited state oxidation product of ABEI. As shown in Fig. S7C,† the CL intensity was positively correlated with the concentration of the dissolved O_2. When $Co^{II}(HQS)_2$ was added into ABEI/GO–KIO_4 system, the CL kinetic curve became sharp (Fig. 5, red line). The duration time of CL emission was greatly reduced to 2 seconds.

The CL mechanism of $Co^{II}(HQS)_2$/ABEI/rGO with KIO_4 was investigated. As shown in Fig. S7C,† the CL intensity was positively correlated with the concentration of the dissolved O_2. It was reported that periodate anion (IO_4^-) could react with the dissolved oxygen in alkaline solution to produce $O_2^{\bullet-}$.[35] When $Co^{II}(HQS)_2$ was added into ABEI/GO–KIO_4 system, the CL kinetic curve became sharp (Fig. 5, red line). The duration time of CL emission was greatly reduced to 2 seconds. Periodate anion could coordinate with the cobalt(II) complex and accompanied by the intramolecular electron transfer to produce cobalt(III) complex, which decomposed to reactive periodate anion radicals (I^{VI}).[36] In this case, it is suggested that IO_4^- reacts with $Co^{II}(HQS)_2$ to follow similar pathways to produce I^{VI}, which facilitated the generation of $O_2^{\bullet-}$ to enhance the CL emission. Meanwhile, when the $Co^{II}(HQS)_2$ was functionalized on the surface of ABEI/GO to form $Co^{II}(HQS)_2$/ABEI/rGO, the CL intensity was further increased. The result indicated that GO also play an important role for the enhanced CL emission, which may be due to that GO stimulate the generation of $O_2^{\bullet-}$, π–C=C$^{\bullet}$ and ABEI$^{\bullet-}$ radicals. The mechanism of $Co^{II}(HQS)_2$/ABEI/rGO–KIO_4 CL system is also summarized as Scheme 2.

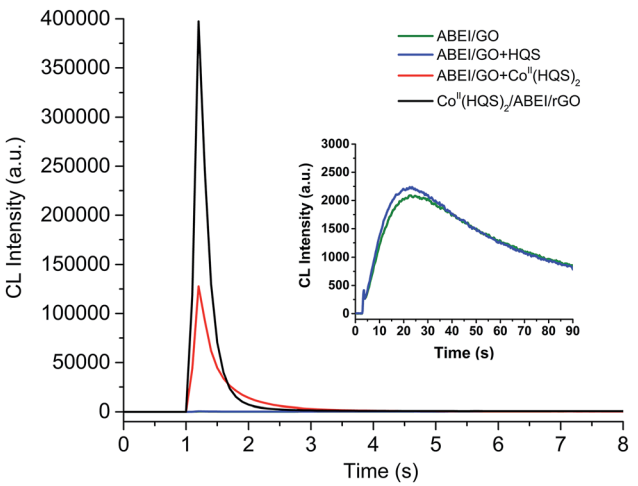

Fig. 5 CL kinetic curves for reaction of ABEI/GO, ABEI/GO mixed with HQS, ABEI/GO mixed with $Co^{II}(HQS)_2$ and $Co^{II}(HQS)_2$/ABEI/rGO with periodate. Reaction conditions: 0.05 mM KIO_4 in 0.05 NaOH.

Thus, the as-prepared $Co^{II}(HQS)_2$/ABEI/rGO could also act as an effective nanocatalytic reaction platform for the heterogenous CL reaction of ABEI with KIO_4 in alkaline solution.

Dilution effect

As shown in Fig. S8,† the as-prepared $Co^{II}(HQS)_2$/ABEI/rGO hybrids was dark brown solution and the hybrids turn to more transparent when diluted. Usually, CL intensity would be declined with the decrease of the CL reagent concentration. However, the CL intensity increased with the increase of dilution times in the range of 1–15 times in $Co^{II}(HQS)_2$/ABEI/rGO–H_2O_2 system and decreased when dilution times further increased (Fig. 6A). The dilution-initiated CL enhancement was also observed in ABEI/GO–H_2O_2, ABEI/GO–O_2 and ABEI/GO–KIO_4 systems (Fig. 6D–F). However, the dilution-initiated CL enhancement was not observed in $Co^{II}(HQS)_2$/ABEI/rGO–O_2 and $Co^{II}(HQS)_2$/ABEI/rGO–KIO_4 system (Fig. 6B and C).

It is well known that GO with the sp^2 domains were excellent fluorescence quenchers and the quenching efficiency of GO was significantly improved after reduction.[37,38] As shown in Fig. 7, the effect of rGO formed *via* reduction of GO by ammonia and hydrazine on the ABEI–H_2O_2 CL system was investigated. The CL intensity (10 s) was quenched by 96.2% and 88.4% in the present of 0.05 mg mL^{-1} and 0.025 mg mL^{-1} rGO, respectively. The results demonstrated that reduced GO could quench effectively the ABEI CL emission and the dilution could decrease the quenching effect of reduced GO.

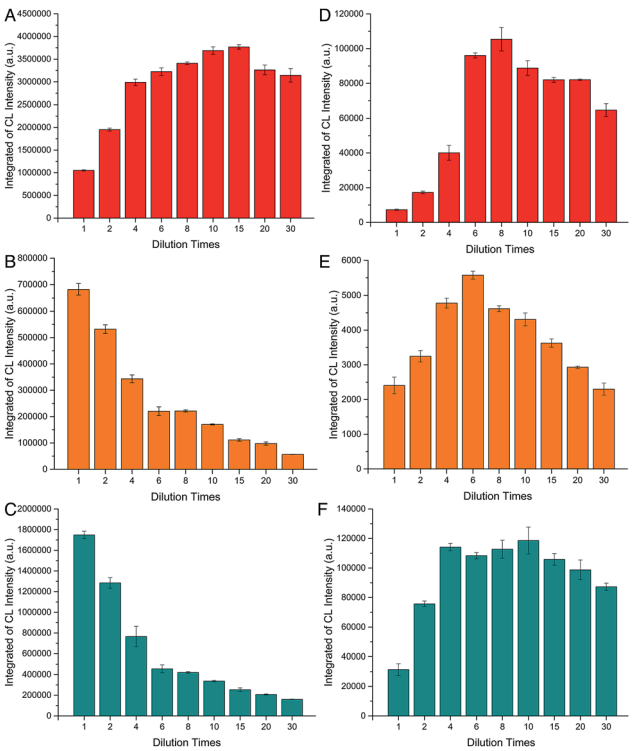

Fig. 6 Effect of dilution on CL intensity of $Co^{II}(HQS)_2$/ABEI/rGO with (A) H_2O_2, (B) O_2, (C) KIO_4, and ABEI/GO with (D) H_2O_2, (E) O_2, (F) KIO_4. Reaction conditions: (A) and (D) 0.1 mM H_2O_2 in 0.01 M NaOH, (B) and (E) 0.1 M NaOH, (C) and (F) 0.05 mM KIO_4 in 0.05 NaOH.

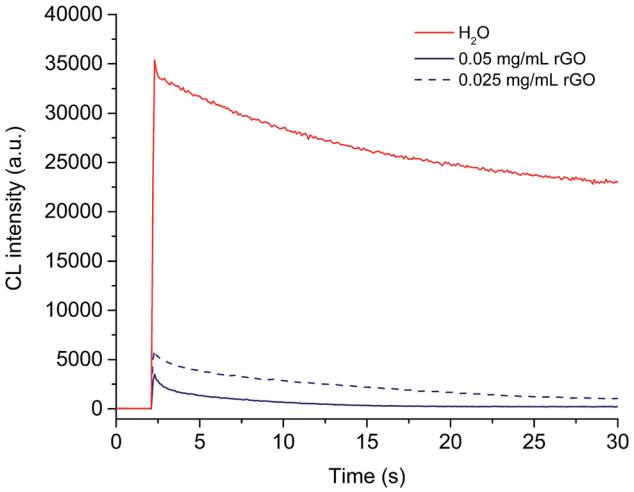

Fig. 7 Effect of rGO formed *via* reduction of GO by ammonia and hydrazine on ABEI–H_2O_2 CL system. Reaction conditions: 0.2 mM ABEI dissolved in H_2O (red curve), 0.05 mg mL^{-1} rGO (blue solid line) and 0.025 mg mL^{-1} rGO (blue dash line), 1 mM H_2O_2 in 0.1 M NaOH.

Therefore, in this case, the dilution of reduced GO in the hybrids to some extent was beneficial to decrease the quenching effect, leading to an increase in CL intensity. This is consistent with CL behavior of ABEI/GO–H_2O_2, ABEI/GO–O_2 and ABEI/GO–KIO_4 systems in the absence of $Co^{II}(HQS)_2$ when they were diluted. When the hybrids contained catalyst $Co^{II}(HQS)_2$, $Co^{II}(HQS)_2$ concentration should also decrease with the increase of dilution times, resulting in a decrease in CL intensity. On the other hand, the dilution would decrease CL quenching effect of reduced GO in the hybrids and increase the CL intensity. As a result, in $Co^{II}(HQS)_2$/ABEI/rGO–O_2 and $Co^{II}(HQS)_2$/ABEI/rGO–KIO_4 system, the CL signal showed a decrease with dilution times (Fig. 6B and 7C), which may be due to that dilution-initiated catalytic decrease dominated the CL behavior. Comparing CL kinetic curve of $Co^{II}(HQS)_2$/ABEI/rGO–H_2O_2 CL system (Fig. 3) with those of $Co^{II}(HQS)_2$/ABEI/rGO–O_2 and $Co^{II}(HQS)_2$/ABEI/rGO–KIO_4 systems (Fig. 4 and 5), the catalytic effect of $Co^{II}(HQS)_2$ in $Co^{II}(HQS)_2$/ABEI/rGO–H_2O_2 CL system is much stronger those in $Co^{II}(HQS)_2$/ABEI/rGO–O_2 and $Co^{II}(HQS)_2$/ABEI/rGO–KIO_4 systems. The dilution-initiated CL enhancement was also observed for $Co^{II}(HQS)_2$/ABEI/rGO–H_2O_2 CL system (Fig. 6A), which may be due to that dilution led to little decrease in catalytic effect and the decrease of CL quenching effect as main factor caused the CL enhancement.

Conclusions

In summary, a novel $Co^{II}(HQS)_2$/ABEI/rGO hybrids was synthesized *via* an economy, facile and simple strategy. ABEI and $Co^{II}(HQS)_2$ were successfully assembled onto the surface of GO by virtue of π–π stacking and coordination. It was found that the as-prepared $Co^{II}(HQS)_2$/ABEI/rGO hybrids could be used as excellent nanocatalytic reaction platforms for chemiluminescence (CL) when reacted with hydrogen peroxide, the dissolved oxygen and periodate in alkaline solution. In these CL reactions, $Co^{II}(HQS)_2$

could catalyze the generation of the reactive radicals on GO surface, such as hydroxyl radicals ($HO^{\bullet}$), superoxide radicals ($O_2^{\bullet-}$), periodate anion radicals (I^{VI}) and π-conjugated carbon radicals (π–C=C$^{\bullet}$), followed by the reaction with ABEI to form ABEI$^{\bullet-}$. ABEI$^{\bullet-}$ would further react with $O_2^{\bullet-}$ to produce strong CL. It was also found that dilution-initiated CL enhancement in $Co^{II}(HQS)_2$/ABEI/rGO–H_2O_2 system but not in $Co^{II}(HQS)_2$/ABEI/rGO–O_2 and $Co^{II}(HQS)_2$/ABEI/rGO–KIO_4 systems. This was attributed to the competition of two processes: dilution decreased reduced GO quenching effect, leading to CL enhancement; dilution decreased $Co^{II}(HQS)_2$ concentration, resulting in a decrease in CL intensity. The former predominanted the CL behavior of $Co^{II}(HQS)_2$/ABEI/rGO–H_2O_2 system, whereas the later predominanted the CL behavior of $Co^{II}(HQS)_2$/ABEI/rGO–O_2 and $Co^{II}(HQS)_2$/ABEI/rGO–KIO_4 systems. This work provides new insight into physicochemical property of functionalized GO hybrids and excellent nanocatalytic platforms for CL reactions, which may find future applications in bioassays, biosensors, bioimaging and microchips.

Acknowledgements

The support of this research by the National Key Research and Development Program of China (Grant No. 2016YFA0201300) and the National Natural Science Foundation of China (Grant No. 21527807 and 21475120) are gratefully acknowledged.

Notes and references

1 H. Kong, D. Liu, S. Zhang and X. Zhang, *Anal. Chem.*, 2011, **83**, 1867–1870.
2 N. Na, S. Zhang, S. Wang and X. Zhang, *J. Am. Chem. Soc.*, 2006, **128**, 14420–14421.
3 C. K. Lim, Y. D. Lee, J. Na, J. M. Oh, S. Her, K. Kim, K. Choi, S. Kim and I. C. Kwon, *Adv. Funct. Mater.*, 2010, **20**, 2644–2648.
4 Y. Su and Y. Lv, *RSC Adv.*, 2014, **4**, 29324–29339.
5 Z. F. Zhang, H. Cui, C. Z. Lai and L. J. Liu, *Anal. Chem.*, 2005, **77**, 3324–3329.
6 H. Chen, F. Gao, R. He and D. Cui, *J. Colloid Interface Sci.*, 2007, **315**, 158–163.
7 R. Gill, R. Polsky and I. Willner, *Small*, 2006, **2**, 1037–1041.
8 S. F. Li, X. M. Zhang, W. X. Du, Y. H. Ni and X. W. Wei, *J. Phys. Chem. C*, 2008, **113**, 1046–1051.
9 H. Cui, W. Wang, C. F. Duan, Y. P. Dong and J. Z. Guo, *Chem.–Eur. J.*, 2007, **13**, 6975–6984.
10 Y. He and R. Peng, *Nanotechnology*, 2014, **25**, 455502–455508.
11 L. U. Syed, L. Z. Swisher, H. Huff, C. Rochford, F. Wang, J. Liu, J. Wu, M. Richter, S. Balivada and D. Troyer, *Analyst*, 2013, **138**, 5600–5609.
12 X. Yang, Y. Guo and A. Wang, *Anal. Chim. Acta*, 2010, **666**, 91–96.
13 M. Liu, H. Zhang, J. Shu, X. Liu, F. Li and H. Cui, *Anal. Chem.*, 2014, **86**, 2857–2861.
14 L. Gao, X. He, L. Ju, X. Liu, F. Li and H. Cui, *Anal. Bioanal. Chem.*, 2016, **408**, 8747–8754.
15 D. R. Dreyer, S. Park, C. W. Bielawski and R. S. Ruoff, *Chem. Soc. Rev.*, 2010, **39**, 228–240.
16 Y. Wang, Z. Li, J. Wang, J. Li and Y. Lin, *Trends Biotechnol.*, 2011, **29**, 205–212.
17 D. Liu, G. Huang, Y. Yu, Y. He, H. Zhang and H. Cui, *Chem. Commun.*, 2013, **49**, 9794–9796.
18 X. Liu, Z. Han, F. Li, L. Gao, G. Liang and H. Cui, *ACS Appl. Mater. Interfaces*, 2015, **7**, 18283–18291.
19 S. Park and R. S. Ruoff, *Nat. Nanotechnol.*, 2009, **4**, 217–224.
20 D. Yang, A. Velamakanni, G. Bozoklu, S. Park, M. Stoller, R. D. Piner, S. Stankovich, I. Jung, D. A. Field and C. A. Ventrice, *Carbon*, 2009, **47**, 145–152.
21 D. Frost, C. McDowell and I. Woolsey, *Mol. Phys.*, 1974, **27**, 1473–1489.
22 A. Das, B. Chakraborty and A. Sood, *Bull. Mater. Sci.*, 2008, **31**, 579–584.
23 W. Shen, Y. Yu, J. Shu and H. Cui, *Chem. Commun.*, 2012, **48**, 2894–2896.
24 K. Soroka, R. S. Vithanage, D. A. Phillips, B. Walker and P. K. Dasgupta, *Anal. Chem.*, 1987, **59**, 629–636.
25 S. B. Raj, P. T. Muthiah, G. Bocelli and L. Righi, *Acta Crystallogr.*, 2001, **57**, 591–594.
26 G. Zhao, J. Li, X. Ren, C. Chen and X. Wang, *Environ. Sci. Technol.*, 2011, **45**, 10454–10462.
27 G. Merenyi and J. S. Lind, *J. Am. Chem. Soc.*, 1980, **102**, 5830–5835.
28 J. Lind, G. MerBnyi and T. E. Erikse, *J. Am. Chem. Soc.*, 1983, **105**, 7655–7661.
29 J. Weiss, *Trans. Faraday Soc.*, 1935, **31**, 1547–1557.
30 J. M. Lin, X. Shan, S. Hanaoka and M. Yamada, *Anal. Chem.*, 2001, **73**, 5043–5051.
31 R. V. Prasad and N. V. Thakkar, *J. Mol. Catal.*, 1994, **92**, 9–20.
32 V. S. Shivankar and N. V. Thakkar, *J. Sci. Ind. Res.*, 2005, **64**, 496–503.
33 L. L. Klopf and T. A. Nieman, *Anal. Chem.*, 1983, **55**, 1080–1083.
34 Q. Lin, A. Guiraúm, R. Escobar and F. Francisco, *Anal. Chim. Acta*, 1993, **283**, 379–385.
35 N. P. Koutsoulis, D. L. Giokas, A. G. Vlessidis and G. Z. Tsogas, *Anal. Chim. Acta*, 2010, **669**, 45–52.
36 M. A. Hussein, A. A. Abdel-Khalek and Y. Sulfab, *J. Chem. Soc., Dalton Trans.*, 1983, **2**, 317–321.
37 J. Kim, L. J. Cote, F. Kim and J. Huang, *J. Am. Chem. Soc.*, 2009, **132**, 260–267.
38 K. P. Loh, Q. Bao, G. Eda and M. Chhowalla, *Nat. Chem.*, 2010, **2**, 1015–1024.